Electron-Beam Lithography and Molecular Liftoff for Directed Attachment of DNA Nanostructures on Silicon: Top-down Meets Bottom-up

Michelle Pillers,[†] Valerie Goss,[‡] and Marya Lieberman*[,†]

[†]Department of Chemistry and Biochemistry, University of Notre Dame, Notre Dame, Indiana 46556, United States
[‡]Department of Chemistry and Physics, Chicago State University, Chicago, Illinois 60628, United States

CONSPECTUS: Our work on lithographic patterning of DNA nanostructures was inspired by a collaboration on molecular electronic devices known as quantum-dot cellular automata or QCA. QCA is a paradigm for computation in which information is transmitted and processed through the interaction of coupled electrical charges or magnetic dipoles. We began to explore the idea of molecular scale QCA and found that *ab initio* methods, a thermodynamic Ising model, and larger scale circuit design work suggested that circuits that did computationally interesting things could function at room temperature if made from molecular QCA cells of chemically reasonable design.

But how could the QCA cells be patterned to form the complex arrays needed for computationally interesting circuitry, and how could those arrays of molecular circuitry be integrated with conventional electronic inputs and outputs? Top-down methods lacked the spatial resolution and high level of parallelism needed to make molecular circuits. Bottom-up chemical synthesis lacked the ability to fabricate arbitrary and heterogeneous structures tens to hundreds of nanometers in size. Chemical self-assembly at the time could produce structures in the right size scale, but was limited to homogeneous arrays. A potential solution to this conundrum was just being demonstrated in the late 1990s and early 2000s: DNA nanostructures self-assembled from oligonucleotides, whose high information density could handle the creation of arbitrary structures and chemical inhomogeneity. Our group became interested in whether DNA nanostructures could function as self-assembling circuit boards for electrical or magnetic QCA systems. This Account focuses on what we learned about the interactions of DNA nanostructures with silicon substrates and, particularly, on how electron-beam lithography could be used to direct the binding of DNA nanostructures on a variety of functional substrates.
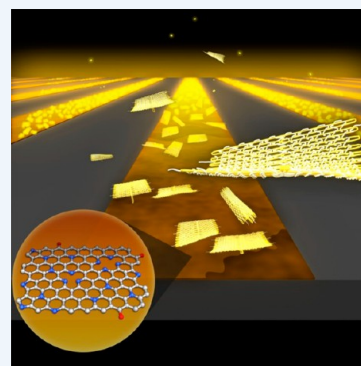
1. INTRODUCTION

Nothing is rich but the inexhaustible wealth of nature. She shows us only surfaces, but she is a million fathoms deep.

Ralph Waldo Emerson.[1]

1.1. DNA Nanostructures

As the other Accounts in this special issue abundantly demonstrate, self-assembly of DNA oligonucleotides can produce highly heterogeneous nanostructures in the 10−100 nm size range.[2] These nanostructures, known as DNA tiles, 2D arrays, scaffolded or templated DNA nanostructures, and DNA origami seamlessly integrate information storage and physical structure.[3] Duplex DNA, which is the basic construction material for DNA nanostructures, may appear to be homogeneous, but small differences in the sequence of base pairs allows for a great deal of structural control. Thus, it is possible to attach oligonucleotides or nanoparticles to specific locations on the surface of a DNA origami that looks like a featureless rectangle. This capability makes DNA nanostructures uniquely suited to bridge between the scale of individual molecules and the scale of lithographic features. DNA nanostructures are indeed "soft" matter, readily draping across underlying surface features, folding, or rolling into tube shapes. The duplex DNA strands interconnected by crossover sites are fluxional in buffer, allowing

DNA strands displayed on one surface of a large flat DNA origami structure to "thread" themselves through to the other side of the origami structure within minutes.[4]

1.2. Properties and Structure of the Default Imaging Surface, Mica

Almost all routine AFM images of DNA nanostructures are obtained on mica substrates. Mica is a layered aluminosilicate with a facile cleavage plane; an atomically flat and clean surface can be produced in the lab with a piece of double sided sticky tape. This cleavage plane of muscovite mica contains 2.2 potassium cations/nm^2,[5] but mica has a negative surface charge density in water because the potassium ions can diffuse away from the mica surface. To help DNA bind, Mg^{2+} is typically[6] used to reverse the negative charge of the mica and bind the phosphate backbone of the DNA.[7] There is a "sweet spot" for optimum binding: Pastre et al. found that the surface binding interaction was maximized if the DNA and mica surface had about the same charge density.[8] DNA origami can be clearly imaged on mica, even in the presence of 200-fold excess of the short

---
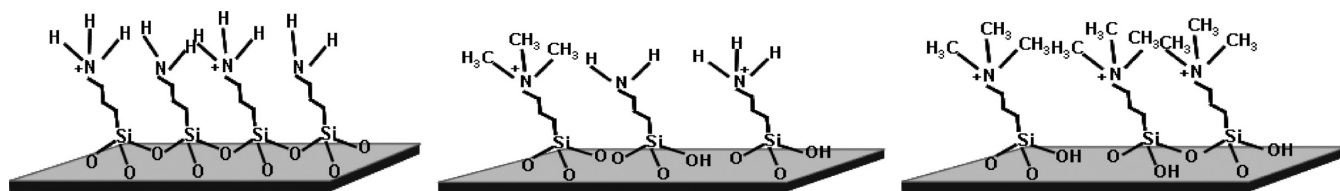
Figure 1. Self-assembled monolayers of pure APTES, mixed APTES and TMAC, and pure TMAC. Reproduced with permission from ref 20. Copyright 2010 SPIE.

oligonucleotides used as "staple" strands in the origami structure; either these short strands do not bind to the surface, or they bind so weakly that the AFM tip easily brushes them aside during image acquisition. Fluid-cell AFM measurements by Loh and Jarvis[9] showed that fewer than half of the potential Mg^{2+} binding sites on freshly cleaved mica were occupied in the presence of 150 mM Mg^{2+}, which would correspond to a surface charge of around 1 charge/nm². This relatively low surface charge would account for why small oligonucleotides do not adhere strongly enough to be imaged by AFM.

1.3. Why the Surface Interaction Matters

Interactions between mica and DNA nanostructures can facilitate self-assembly of very large tile arrays with low defect density.[10,11] This binding interaction can force a nanostructure that in solution is curled like a potato chip[12] to lie flat on the surface, or it can unfold or crush a desired three-dimensional shape.[13] It would be advantageous to be able to control the strength of surface binding.

2. DNA NANOSTRUCTURES ON SILICON

2.1. Small DNA Nanostructures Bind to Cationic Monolayers on Silicon

The stability of the Seeman–Winfree DNA tile arrays, published in 1998, was striking.[14] After magnesium-mediated binding to mica, these structures could be imaged by contact mode AFM under organic solvents like isopropanol or in air, surviving strong tip–sample contact forces and the drag exerted by the water meniscus around the tip. We decided to explore tile arrays as potential "circuit boards" for quantum-dot cellular automata (QCA). A diamond-shaped four-tile assembly with dimensions of 8 nm × 37 nm was designed.[15] Each tile in the four-tile raft had two sticky-end overlaps with neighboring tiles.

We knew that silicon oxide had a lower surface charge than mica, so we looked for alternatives to magnesium-mediated binding. The strong surface binding interaction between polylysine functionalized mica and DNA[16] suggested that cationic self-assembled monolayers of APTES on silicon might do the job. Our group already had considerable experience using aminopropyltriethoxysilane (APTES) as a priming monolayer for formation of layered materials,[17] and we hoped we might be able to rinse away the sodium, potassium, and magnesium buffer ions in the DNA deposition solution; most clean rooms are strict about keeping these species away from the silicon processing areas because they can alter the electronic properties of CMOS structures; for example, sodium forms efficient midbandgap traps in silicon.[18]

Because the DNA nanostructures we were using were just 2 nm in height, it was important for the APTES SAMs to be very smooth. Although APTES is hydrolytically unstable, we found that by using fresh APTES and high-purity water and by completing the SAM deposition within 30 min, APTES surfaces with root-mean-square (RMS) roughness over 1 um² of less than

0.15 nm were obtained. APTES was deposited from aqueous solution, in which the trialkoxysilane is known to hydrolyze and form aggregates, rather than from dry organic solvents, because we wished to form patterned APTES monolayers, and the patterning process was only compatible with aqueous solutions of SAM precursors.

The four-tile raft was small enough to allow assembly to be followed by gel electrophoresis and large enough (barely) to give visibly elliptical images in the AFM after deposition on APTES-treated silicon. Importantly, repeated imaging in air gave identical images; the DNA rafts did not move under the influence of the tip. High densities of four-tile rafts could be deposited on the APTES, although their small size made it difficult to count them.

2.2. Tuning the Charge Density of Cationic Monolayers

When Rothemund published the DNA origami technique in 2006,[19] we gladly switched to these much larger and easier to image DNA nanostructures. Like tile arrays and the four-tile rafts, DNA nanostructures bind poorly to the background silicon oxide, which bears a much lower surface charge than mica. The anionic charge on SiO_2 originates from deprotonation of silanol groups; the density of silanol groups on an oxide surface is strongly dependent upon the sample history. Chemical cleaning, thermal annealing, and plasma etching all affect the ratio of silanol and silyl ether functional groups exposed on the surface. At pH 8.0 and 12 mM Mg^{2+}, we typically see fewer than one origami per square micrometer on native oxides.

We used mixed monolayers of APTES and trimethoxysilyl-propyl-N,N,N-trimethylammonium chloride (TMAC) to tune the surface charge of cationic siloxane SAMs on silicon.[20] A secondary benefit of this approach is that the ionic strength and magnesium concentration, which both strongly influence the structure and melting point of duplex DNA, can be held constant. TMAC and APTES (Figure 1) are both moderately hydrophilic; the advancing water contact angle for a TMAC SAM is $56° \pm 7°$, while that for APTES is $65° \pm 5°$. However, TMAC cannot act as a H-bond donor or acceptor, and its positive charge does not depend on its protonation state.

The monolayer composition and surface charge of each mixed monolayer could be measured by X-ray photoelectron spectroscopy (XPS) as seen in Figure 2. To determine the absolute coverage, the N/Si ratio was compared with that measured for a 7 Å thick monolayer of APTES deposited on native oxide from dry toluene (N/Si = 0.040 ± 0.0066). APTES forms SAMs with a cross-sectional area of 25 Å²/molecule. The N/Si ratio for a full monolayer of TMAC indicated a nitrogen atom coverage just $40\% \pm 14\%$ of the value for full coverage APTES, corresponding to a surface area of 62 ± 30 Å² per TMAC molecule. The cross-sectional area of tetramethylammonium is 60 Å²,[21] so the TMAC monolayer appears to be well packed. We found that, as is common for mixed monolayer depositions, the composition of the deposition solution did not track exactly with the
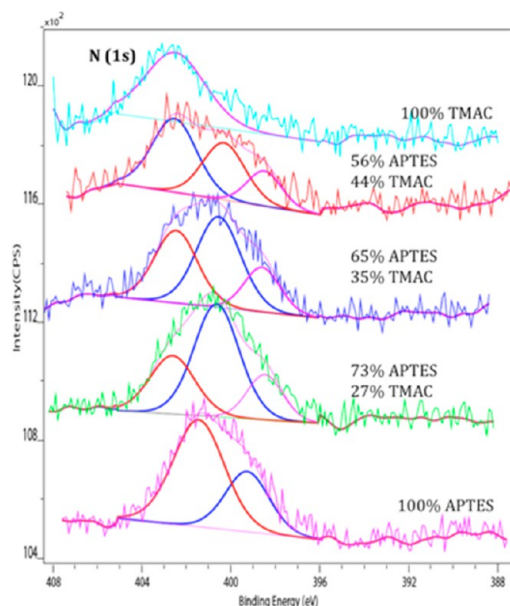
Figure 2. XPS spectra of pure and mixed monolayers of APTES and TMAC on Si[100]. Solid curves show peak fits. Reproduced with permission from ref 20. Copyright 2010 SPIE.

composition of the monolayer; for example, a 75% TMAC/25% APTES deposition solution gave a monolayer that was just 44% TMAC. Optimal binding of DNA origami was observed for SAMs with TMAC concentrations of 100% to 40%, corresponding to surface charges in the range of 0.75–1.5 charges/nm^2.

Binding densities of around 110 origami/um^2 with a binding selectivity of 50:1 were obtained on APTES SAMs and 120 origami/um^2 with a binding selectivity of 120:1 on TMAC SAMs.[22]

3. MOLECULAR LIFTOFF[23]

We had begun to explore the use of electron-beam lithography (EBL) as a molecular patterning tool as part of our molecular electronics work, and it seemed like a natural match to the task of guiding the deposition of DNA nanostructures on silicon. The native oxide on a silicon chip is covered with a 30–60 nm thick film of poly(methyl methacrylate) (PMMA), which is patterned by exposure to a 20–100 keV electron beam. Although the primary electron beam is usually below 5 nm in diameter, hundreds of secondary electrons are generated from each primary electron when the beam hits the PMMA, and a region

20–30 nm wide is exposed to considerable damage and fragmentation. The damaged polymer film is removed, revealing clean silicon oxide ready for whatever material deposition step the user wishes, such as metal evaporation. In the final stage of processing, the unexposed PMMA is lifted off with acetone.

As part of a study directed at fabrication of arrays of molecular quantum-dot cellular automata, we had shown that the cationic Creutz–Taube (CT) molecule, $[(NH_3)_5Ru(pyrazine)Ru(NH_3)_5]^{5+}$, could be directly patterned on smooth silicon oxide surfaces by "molecular liftoff". The formation of a monolayer from aqueous deposition of CT ions was a surprising result because unmodified PMMA is quite hydrophobic, and penetration of a water droplet into a narrow trench would not be favorable. Since water was obviously penetrating into the trenches, the damaged PMMA must contain enough oxygenated functional groups to be hydrophilic. In a follow-up study, we found that cold development conditions were much more selective for dissolution of highly damaged PMMA, which allowed use of higher beam doses and formation of even narrower tracks, just 4–10 nm wide, in a 60 nm thick PMMA film.[24,25] Citrate-stabilized 5.7 nm diameter gold nanoparticles were deposited in a 10 nm-width trench; the particles formed a single-particle line, demonstrating that the trenches penetrated down to the silicon surface without much undercut. These example of "molecular liftoff" of molecules and colloidal particles suggested that other aqueous materials, such as biomolecules, could be deposited into EBL trenches.[26]

3.1. Molecular Liftoff of Proteins and Small DNA Nanostructures

An early attempt to use the molecular liftoff technique to pattern first poly(lysine) and then four-tile DNA rafts into 100 nm wide trenches in PMMA failed, because liftoff with methylene chloride produced a very rough surface coated with 1–10 nm particles. Switching from poly(lysine) to APTES solved this problem, leading to the process shown in Figure 3.

Each APTES molecule in a self-assembled monolayer is covalently linked to the substrate and to its neighbors in a two-dimensional siloxane network. Once this network formed inside the PMMA trenches, exposure to solvents powerful enough to lift off the PMMA had no effect on the SAM. APTES SAMs patterned by molecular liftoff were stable to Soxhlet extraction with boiling acetone or dichloromethane, as well as 30 min sonication in these solvents. The APTES SAMs served to anchor *Salmonella* phage P22 Tailspike protein.[27] If a moderately anionic protein such as Tailspike could bind to cationic APTES features and apparently retain its structure, then strongly anionic DNA
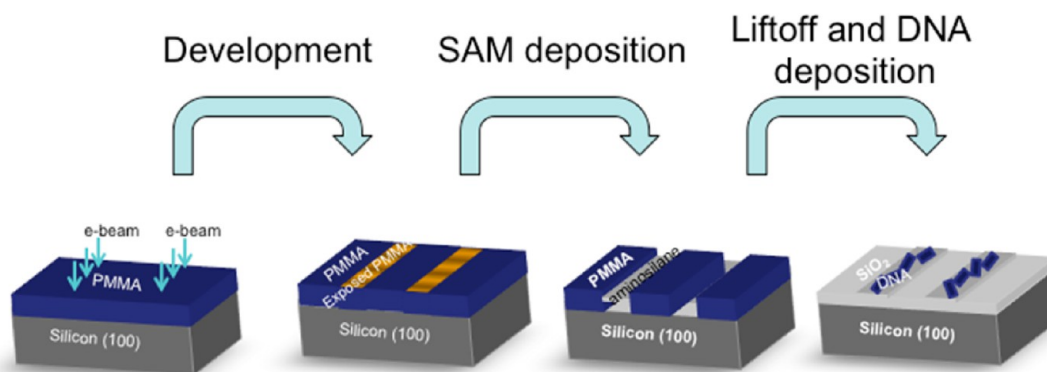

Figure 3. Molecular liftoff process flow for deposition of DNA nanostructures.

nanostructures might also adhere to cationic SAMs deposited on silicon substrates. Preliminary studies of the attachment of four-tile raft structures on 100 nm wide APTES lines showed a height increase of 2.7 nm and such dense binding that it was difficult to resolve one raft from the next, given the tip-induced broadening typical for AFM.[28]

We wanted to gauge the strength of the interaction between the four-tile rafts and the APTES surface. One indication of strong surface binding is jamming behavior.[29] If an object binds randomly and irreversibly to a surface, it cannot access the most efficient packing arrangement, and the final coverage will be lower than the theoretical maximum coverage. For ovals with an aspect ratio of 4:1, like our four-tile rafts, the jamming limit will be reached at a coverage of 0.55; the theoretical maximum coverage (with reorientation) is 0.95. For the four-tile rafts binding to 60 nm wide APTES lines,[30] we observed a saturation coverage of 0.42 after 4 h, suggesting that the rafts were "jammed" on the APTES surface.

As a further test to see whether the DNA nanostructures were kinetically trapped on the surface, we studied their orientation on narrow APTES features. Narrow tracks of APTES should provide maximal binding energy for 8 nm × 37 nm rafts oriented with their major axis parallel to the APTES line. If the rafts were capable of reorientation after binding to the surface, they should rotate to align their major axis along the direction of the APTES stripe, so that the entire raft could interact with that cationic feature. Rafts bound to 17 nm APTES lines with a selectivity of more than 30:1 over background binding to SiO$_2$, as seen in Figure 4.[31] However, the direction of the major axis of the ovals
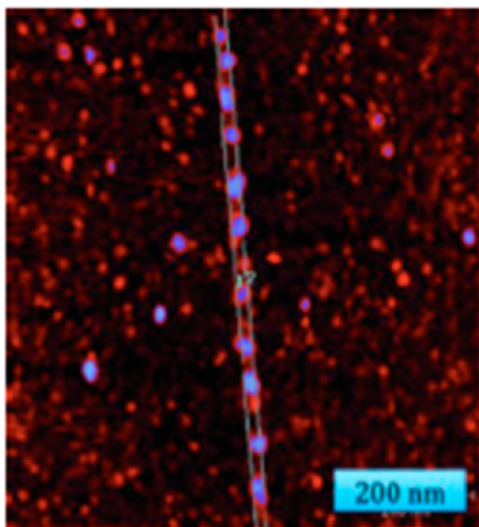
Figure 4. Four-tile DNA rafts bound to a 17 nm wide line of APTES on SiO$_2$. Noncontact AFM in air. Reproduced with permission from ref 31. Copyright 2010 American Chemical Society.

was random with respect to the direction of the APTES stripe. As in the earlier experiments, the rafts appear to be jammed on the APTES surface.

The molecular liftoff method was used to make arrays of APTES anchor pads 35–40 nm in diameter. The binding of the rafts to the APTES anchor pads could be clearly observed due to the increase in cross-sectional height from 0.7 nm for plain APTES, to 1.9 ± 0.9 nm for a bound raft. Each anchor pad could hold only one or two DNA rafts, so adhesion of DNA nanostructures to the surface could be treated using a simple

two-state model of binding. A lower bound for the binding constant K_b can be expressed as

$$K_b = \frac{SD}{S}\frac{1}{[D]} \tag{1.1}$$

where S represents the number of surface binding sites, $[D]$ is the solution concentration of DNA rafts, and SD represents the number of surface binding sites occupied by a DNA raft. The calculated value of $K_b = (3-7) \times 10^7$ M^{-1} corresponds to a free energy of binding between each DNA raft and its anchor pad, $\Delta G_b^\circ = -RT \ln K_b$ as a minimum of −11 kcal/mol (−43 kJ/mol).

### 3.2. Molecular Liftoff of DNA Origami

Molecular liftoff was used to fabricate 90 nm × 70 nm APTES anchor pads (Figure 5), and eq 1.1 was used to calculate the
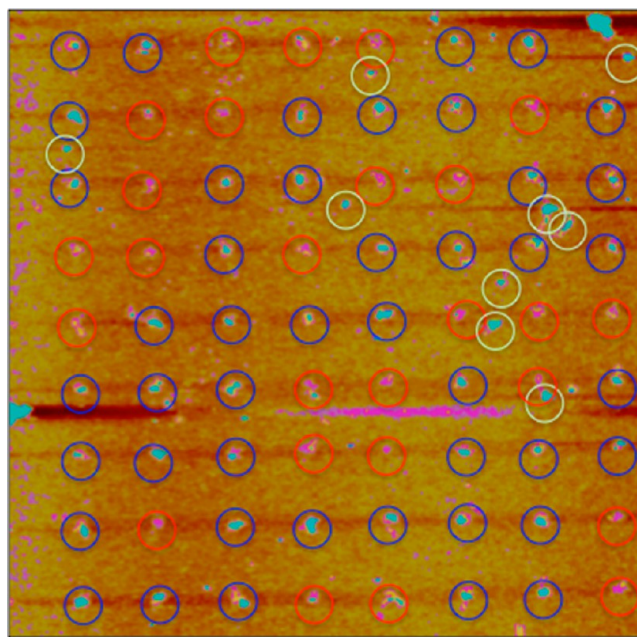

Figure 5. Array of 71 APTES anchor pads after 12 h exposure to 2 nM DNA origami solution; 45 pads are occupied by a single origami (blue circles), 26 pads are empty (red circles), and 9 origami bound to background (white circles). AFM image in air, 5 μm scale. Reproduced with permission from ref 20. Copyright 2010 SPIE.

binding constant (K_b) for the DNA origami attachment as 9×10^8 M^{-1}.[32] This is about 20 times larger than the K_b for DNA rafts binding on APTES nanodots that Gao et al. obtained. The area of the four-tile rafts is 300 nm^2, while the area of the DNA origami rectangle is 6300 nm^2, so K_b appears to scale with area. The high binding affinity of DNA nanostructures for APTES was also noted by the Wind group, which used nanoimprint lithography to make APTES binding pads to trap DNA origami at desired locations.[33]

Both the "jamming" behavior of DNA nanostructures on wide APTES anchor pads and the inability of narrow APTES anchor pads to orient the DNA nanostructures indicate that the H-bonding and electrostatic interaction between the DNA nanostructures and the cationic regions is, if anything, too strong: once a DNA nanostructure touches down on the charged area, it cannot slide along the surface, even to attain a thermodynamically more stable orientation. We turned to TMAC to reduce the surface binding forces.
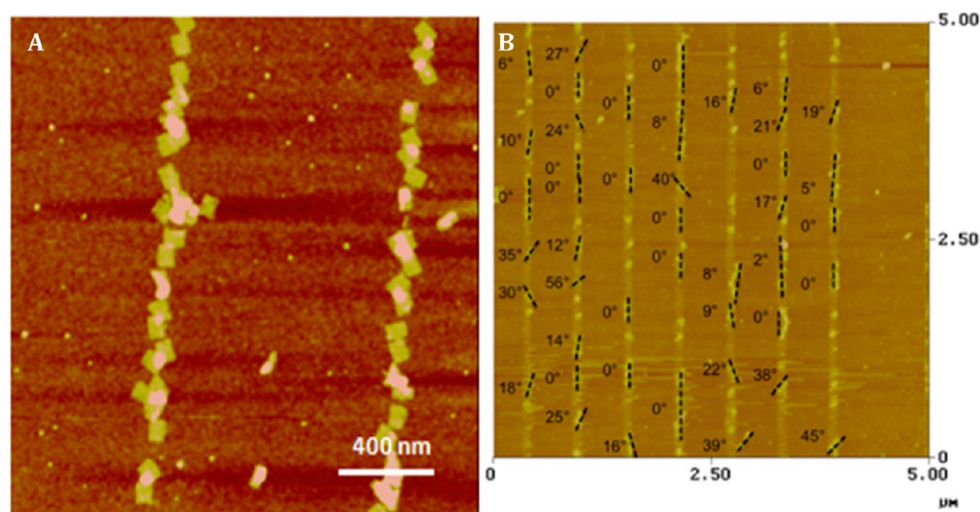
Figure 6. Orientation of DNA origami on TMAC tracks: (A) poorly oriented DNA origami with destructured edges (to discourage π stacking) on 60 nm TMAC lines; (B) well oriented DNA origami oligomers on 70 nm wide TMAC SAMs on HMDS/silicon. Reproduced with permission from ref 32. Copyright 2012 University of Notre Dame.
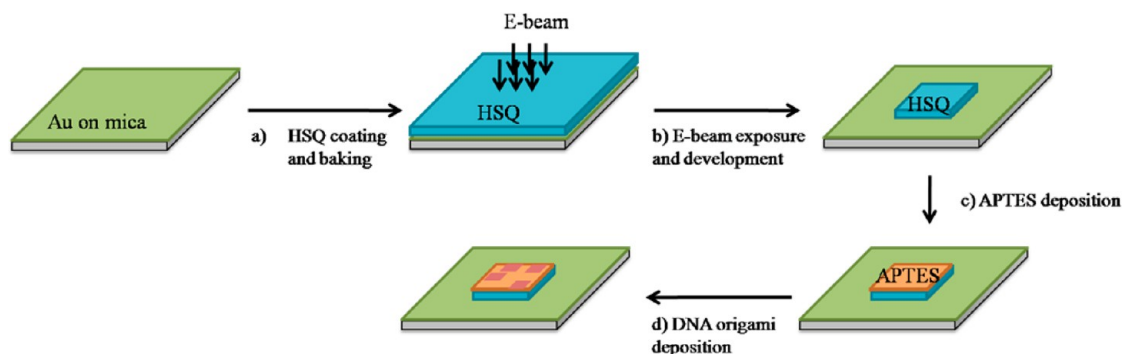
Figure 7. Attachment of DNA origami on APTES treated HSQ patterns on Au/mica: (a) 20 nm Ti and 200 nm Au were evaporated on mica, and HSQ was spun on and baked; (b) HSQ was exposed with area dose of 1600 μC/cm^2 and developed; (c) APTES was deposited for 15 min in water; (d) DNA deposition, washing, and drying. Reproduced with permission from ref 38. Copyright 2012 AIP Publishing LLC.

TMAC tracks 70 nm wide were fabricated, and very high coverages and binding selectivities were obtained on the tracks (Figure 6A). The origami were not strongly oriented, which we think is because the 70 nm × 100 nm rectangle was just not very anisotropic. The ends of a DNA helix are hydrophobic, and when a DNA origami contains many such ends aligned along one edge of the DNA origami, then the edges of two origami can π stack in solution.[34] This phenomenon can produce quite long oligomers of origami that deposit on surfaces as long ribbons. When a rectangular origami design optimized for π stacking was deposited, many such oligomers were observed binding to the 70 nm wide TMAC tracks (Figure 6B), and the average angle between the long axis of each origami oligomer and the track axis was $13° \pm 15°$, indistinguishable from zero. This suggests that the anisotropic origami oligomers were able to reorient on the patterned surface.

Kershner et al. reported the adhesion of individual triangular DNA origami structures to plasma-etched diamond like carbon in the presence of 100 mM magnesium.[35] Rinsing the substrate with water or removing it from the buffer dislodged the origami, a result also observed with magnesium-mediated attachment to plasma-etched silicon oxide. The magnesium-bound patterned origami could be successfully transferred to air by successive washing steps in ethanol/water mixtures, which dehydrated the surface in a controlled manner.[36] In contrast, cationic SAM anchor pads are covalently attached to the SiO$_2$ substrate, so the DNA origami are persistently attached and retain their structures even after rinsing with buffer or DI water and drying.

### 3.3. Alternatives to PMMA for Molecular Liftoff

Hydrosilsesquioxane (HSQ) is a negative-tone EBL resist; the electron beam cross-links and stabilizes the resist film, instead of damaging it and rendering it easy to remove, as for PMMA. HSQ can be applied to nonreactive substrates like gold, graphite, or even plastics.[37] Cross-linked HSQ is chemically similar to SiO$_2$, and indeed, we found that it could be treated with APTES to promote adhesion of DNA origami, as shown schematically in Figure 7.[38] This result is significant because the processing steps for HSQ are mild, so it could provide a route to multilevel patterning of DNA nanostructures.

3.4. Modeling the Binding of Origami to Mica and to Cationic Monolayers on Silicon

The binding characteristics of rectangular DNA origami on a surface can be modeled using a random sequential adsorption model (RSA)[39] or as a Langmuir isotherm.[40] The RSA model assumes that (1) hard objects are randomly placed on a surface in sequential order, (2) last placed overlapping objects are removed from the surface upon landing, (3) once bound to the surface the

objects do not unbind, and (4) the jamming limit, θ_j, is reached when all space is covered without overlapping objects. In contrast, the Langmuir model assumes that adsorption and desorption occur at specific surface sites, which do not interfere with one another, allowing 100% coverage. In the simplest Langmuir model, all the surface sites have a uniform structure. We made coverage vs time measurements for deposition of a standard rectangular DNA origami on three different surfaces, mica, APTES, and TMAC (Figure 8),[41] and compared the
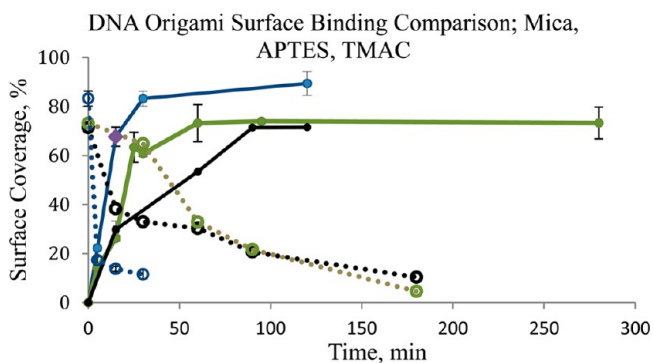
Figure 8. DNA origami binding to mica, APTES, and TMAC SAMs. Coverages measured by noncontact mode AFM in air, after blowing deposition solution from chip; error bars represent ±1SD, n = 3. MICA = blue lines, APTES = olive lines, TMAC = black lines. Solid lines correspond to adsorption, and dashed lines to desorption. Reproduced with permission from ref 41. Copyright 2012 University of Notre Dame.

experimental saturation binding to predictions based on the RSA model, and we fit the adsorption and desorption kinetics to a Langmuir binding model using techniques described by the Harris group.[42,43]

For a 70 nm × 100 nm origami, the theoretical jamming limit, θ_j, is 0.552.[44] On all three surfaces, this jamming limit was exceeded; for mica, it was 0.83 ± 0.03, for APTES, it was 0.73 ± 0.08, and for TMAC, it was 0.71 ± 0.05. However, the pathway to saturation binding on mica was qualitatively different from that on APTES and TMAC. On mica, the adsorption rate was higher than on either of the SAMs, and the highest coverage samples contained very few overlapping or folded origami. Instead, as the coverage increased beyond the theoretical jamming limit of 0.55, the origami reoriented so adjacent origami could achieve better packing. In contrast, the TMAC and APTES samples showed single-layer binding up to a coverage value of about 0.55, but after that many overlapping origami were present (Figure 9). In these samples, the origami cannot reorient, so new origami may stick to
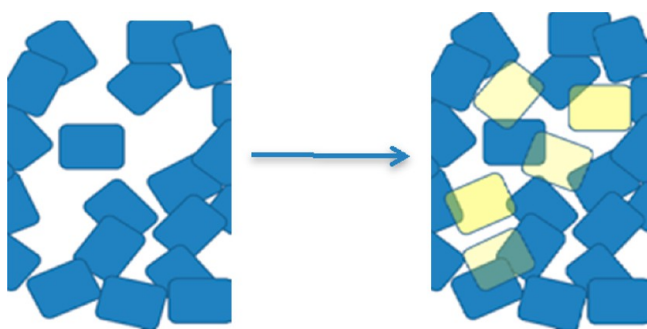
Figure 9. DNA origami binding on a "jammed" surface. Reproduced with permission from ref 41. Copyright 2012 University of Notre Dame.

a small exposed portion of the cationic SAM, and then the rest of the origami must overlap on top of previously deposited origami.

The difference between magnesium-mediated binding to mica and SAM-mediated binding to silicon oxide was also evident in the desorption kinetics. DNA origami desorption from mica occurred in two phases: an initial fast phase removed two-thirds of the bound DNA origami within 5 min, while residual origami continued to desorb at a much slower rate. Origami on APTES and TMAC surfaces desorbed at the same rate, which matched the slow phase of mica desorption.

The commercial availability of fast scanning AFM instruments[45] now allows reorientation of origami on mica to be directly observed; Figure 10 shows two images from a video of the reorientation of a cross-shaped origami[46] in buffer solution as it joins a growing chain on a mica surface.[47]

### 3.5. Directed Binding of DNA Nanostructures to Graphene

Graphene has attracted much attention for nanoelectronic applications, but adsorption of biological molecules to graphene is difficult due to the hydrophobic nature of this substrate.[48] DNA origami do not adhere well to pristine graphene, but they bind well to chemically modified graphene substrates.[49] We found that graphene oxide (GO) flakes functionalized with aminopropyl trimethoxysilane (APTS) were found to immobilize DNA origami rectangles via the previously described electrostatic interaction between the negatively charged DNA origami and the cationic APTS. Photolithography and chemical modification techniques were used to pattern various graphene-based substrates: graphene oxide (GO), reduced graphene oxide (rGO), nitrogen-doped reduced graphene oxide (NrGO), and pristine CVD deposited graphene (Figure 11). Only the GO and NrGO contain functional groups that can anchor a self-assembled monolayer of APTS, and these were the surfaces that anchored high densities of DNA origami.

## 4. A GLANCE TO THE FUTURE: DNA ORIGAMI AS LITHOGRAPHIC PROCESS AIDS

DNA origami are self-assembling materials that might play an active role in conventional processing of semiconductor chips. DNA nanostructures can be metallized by electroless deposition or by thermal evaporation, leading to conductive nanowires, although often the metallic wires are significantly wider than the DNA templates.[50,51] It is also possible to attach carbon nanotubes on DNA origami with controlled orientation (e.g., lengthwise vs widthwise), which can be used to construct crossbar structures.[52] The Norton group recently extended this idea to assemble and align pairs of single-walled carbon nanotubes.[53]

Using DNA origami as a resist material or source of dopant atoms is also feasible. Liu's group found that DNA origami and duplex DNA strands deposited on 300 nm thick silicon oxide films could act as either positive or negative tone resists for HF etching of the SiO_2.[54] Trenches 2–3 nm deep were obtained under conditions of high humidity, where the HF was concentrated near the DNA, and ridges 2–3 nm in height were observed under conditions of low humidity, where the DNA shielded the underlying oxide from the HF etchant. It would be interesting to measure the amount of undercut for these positive and negative tone resists and to see if they could be used (perhaps on a thin native oxide) as masks for further processing of the silicon surface.

Another possibility is to directly use atoms from a DNA nanostructure as dopants in the processing of a semiconductor.
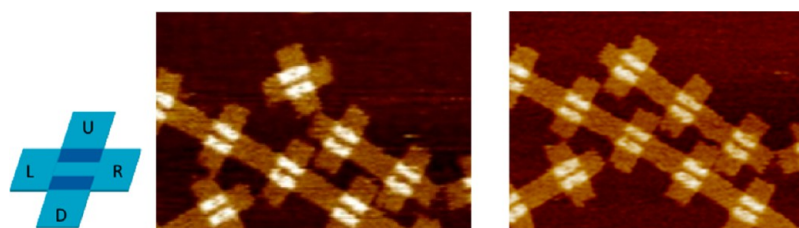
Figure 10. Cross-shaped origami, imaged by noncontact mode AFM in buffer, reorients and binds to growing "train" of origami within 4 s. Images were kindly provided by Michael Norton and Masudur Rahman, Marshall University.
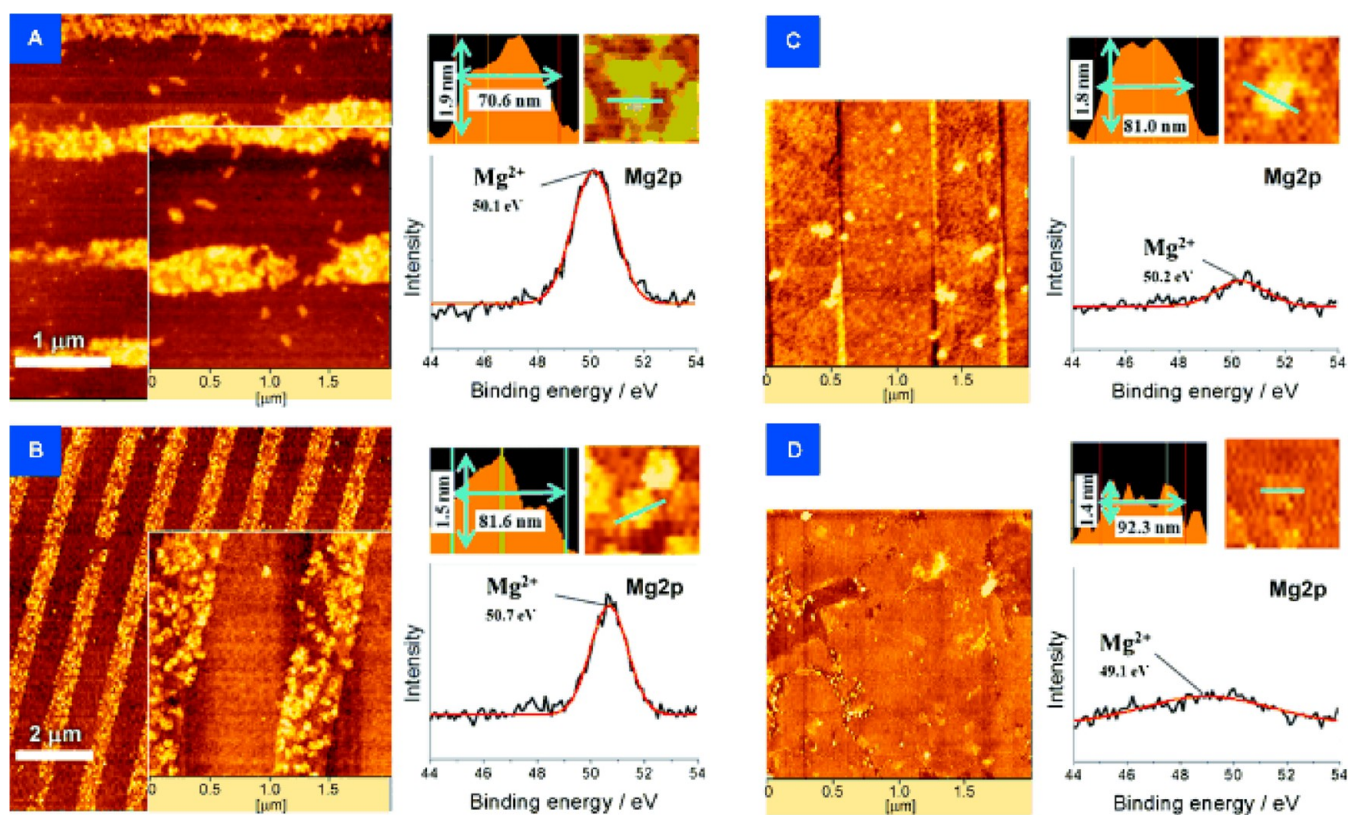
Figure 11. AFM images and XPS spectra (Mg_{2p} region) for DNA origami deposited on (A) GO, (B) NrGP, (C) rGO, and (D) graphene grown with CVD. Reproduced with permission from ref 49. Copyright 2012 Wiley.
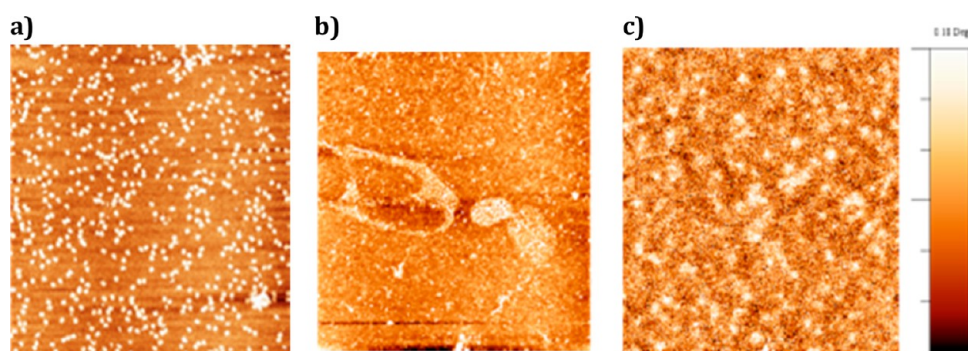
Figure 12. Burn-in doping creates conductive areas on a p-doped silicon wafer: (a) origami before burn-in ($5 \times 5 \ \mu m^2$ image, vertical scale 0−5 nm); (b) AFM topographic image after burn-in and etching ($5 \times 5 \ \mu m^2$ image; vertical scale 0−1.37 nm; DNA would be at least 1.5 nm); (c) electrostatic force microscopy (EFM) image of region in panel b. The bright areas average 200 nm in diameter and are more conductive than the background. Reproduced with permission from ref 41. Copyright 2012 University of Notre Dame.

There is considerable precedent for driving in atoms from a surface layer via rapid thermal processing to form doped regions. Sivoththaman et al.[55] showed that phosphorus diffusion from a thin film of phosphoric acid resulted in shallow but very high doping concentrations (between 10^{19} and 10^{20} cm^{-3}). We are building on this by using DNA origami to directly lay out n$^+$

1765

dx.doi.org/10.1021/ar500001e | *Acc. Chem. Res.* 2014, 47, 1759−1767

regions and n/p junctions on silicon.[56] As a test of the general approach, we used rapid thermal processing to "burn in" phosphorus atoms from DNA origami on APTES-treated silicon (Figure 12a). The DNA origami were capped with a thick film of SiO_2, thermally annealed, and etched in 10% HF to remove the silicon oxide cap and any remaining organic residues. AFM (Figure 12b) showed no trace of the original rectangular DNA origami in the topographic images, but electrostatic force microscopy (Figure 12c) showed the appearance of many conductive patches approximately 200 nm in size.

■ AUTHOR INFORMATION

Corresponding Author

*E-mail: mlieberm@nd.edu.

Notes

The authors declare no competing financial interest.

Biographies

Michelle Pillers is a graduate student in Dr. Lieberman's group in the Department of Chemistry and Biochemistry at the University of Notre Dame. She earned a B.S. in Chemistry and a B.A. in Biology from Southern Methodist University in Dallas, TX. Her current research focuses on using DNA origami for nanoelectronic applications.

Valerie Goss is an assistant professor of Chemistry at Chicago State University (1996 B.S.). She earned a M.S. from Loyola University at Chicago in Biochemistry. She completed a M.S. in Geological Sciences at the University of Notre Dame followed by a doctoral degree in Chemistry in 2012. Her thesis focused on understanding the binding kinetics of DNA origami on mica and modified silicon surfaces.

Marya Lieberman is an associate professor in the Department of Chemistry and Biochemistry at the University of Notre Dame. Prior to joining the faculty in 1996, she worked with Prof. Tomikazu Sasaki on *ab initio* design of artificial proteins at the University of Washington in Seattle, and then took an NSF Postdoctoral Fellowship at Caltech in the group of Prof Nathan Lewis. Her research interests include surface and analytical chemistry, and she has experience in formation and characterization of unusual self-assembled monolayers, X-ray photoelectron spectroscopy, and high-resolution electron beam lithography, in addition to phthalocyanine and coordination chemistry.

■ ACKNOWLEDGMENTS

■ REFERENCES

(1) Edward, T. *A Dictionary of Thoughts: Being a Cyclopedia of Laconic Quotations from the Best Authors of the World, Both Ancient and Modern*; Cassel Publishing Co.: New York, 1891; p 373.

(2) Shih, W. M.; Lin, C. Knitting complex weaves with DNA origami. *Curr. Opin. Struct. Biol.* **2010**, *20*, 276−282. Seeman, N. C.; Belcher, A. M. Emulating biology: Building nanostructures from the bottom up. *Proc. Natl. Acad. Sci. U.S.A.* **2002**, *99*, 6451−6455 S2.

(3) Lieberman, M. DNA Nanostructures. In *Nanobiotechnology Handbook*; Xie, Y., Ed.; CRC Press/Taylor & Francis: Boca Raton, FL, 2013; Chapter 1, pp 3−30.

(4) Wu, N.; Czajkowsky, D. M.; Zhang, J.; Qu, J.; Ye, M.; Zeng, D.; Zhou, X.; Hu, J.; Shao, Z.; Li, B.; Fan, C. Molecular threading and tunable molecular recognition on DNA origami nanostructures. *J. Am. Chem. Soc.* **2013**, *135* (33), 12172−12175.

(5) Schlegel, M. L.; Nagy, K. L.; Fenter, P.; Cheng, L.; Sturchio, N. C.; Jacobsen, S. D. Cation sorption on the muscovite (0 0 1) surface in chloride solutions using high-resolution X-ray reflectivity. *Geochim. Cosmochim. Acta* **2006**, *70*, 3549−3565.

(6) Vesenka, J.; Guthold, M.; Tang, C. L.; Keller, D.; Delaine, E.; Bustamante, C. Substrate preparation for reliable imaging of DNA molecules with the scanning force microscope. *Ultramicroscopy* **1992**, *42*, 1243−1249.

(7) Bustamante, C.; Vesenka, J.; Tang, C. L.; Rees, W.; Guthold, M.; Keller, R. Circular DNA-molecules imaged in air by scanning force microscopy. *Biochemistry* **1992**, *31*, 22−26.

(8) In addition to Bustamante et al., see: Pastré, D.; Piétrement, O.; Fusil, S.; Landousy, F.; Jeusset, J.; David, M.; Hamon, L.; Le Cam, E.; Zozime, A. Adsorption of DNA to mica mediated by divalent counterions: A theoretical and experimental study. *Biophys. J.* **2003**, *85* (4), 2507−2518.

(9) Loh, S. H.; Jarvis, S. Visualization of ion distribution at the mica-electrolyte interface. *Langmuir* **2010**, *26*, 9176−9178.

(10) Sun, X.; Ko, S. H.; Zhang, C.; Ribbe, A. E.; Mao, C. D. Surface-mediated DNA self-assembly. *J. Am. Chem. Soc.* **2009**, *131*, 13248−13249.

(11) Hamada, S.; Murata, S. Substrate-assisted assembly of interconnected single-duplex DNA nanostructures. *Angew. Chem., Int. Ed.* **2009**, *48*, 6820−6823.

(12) Kim, D. N.; Kilchherr, F.; Dietz, H.; Bathe, M. Quantitative prediction of 3D solution shape and flexibility of nucleic acid nanostructures. *Nucl. Acids. Res.* **2012**, *40* (7), 2862−2868.

(13) Endo, M.; Hidaka, K.; Sugiyama, H. Direct AFM observation of an opening event of a DNA cuboid constructed via a prism structure. *Org. Biomol Chem.* **2011**, *9*, 2075−2077.

(14) Winfree, E.; Liu, F.; Wenzler, L. A.; Seeman, N. C. Design and self-assembly of two-dimensional DNA crystals. *Nature* **1998**, *394*, 539−544.

(15) Sarvewsaran, K.; Huber, P.; Lieberman, M.; Russo, C.; Lent, C. S. Nanometer Scale Rafts Built from DNA Tiles. *Proc. 3rd IEEE Conf. Nanotechnol.* **2003**, *2*, 417−420.

(16) Niwa, M.; Morikawa, M.; Yagi, K.; Higashi, N. Interaction between polylysine monolayer and DNA at the air-water interface. *Int. J. Biol. Macromol.* **2002**, *30*, 47−54.

(17) Wang, X. J.; Lieberman, M. Zirconium-phosphonate monolayers with embedded disulfide bonds. *Langmuir* **2003**, *19*, 7346−7353.

(18) Sze, S. M.; Ng, K. K. *Physics of Semiconductor Devices*, 3rd ed.; Wiley: New York, 2007; pp 213−224.

(19) Rothemund, P. W. K. Folding DNA to create nanoscale shapes and patterns. *Nature* **2006**, *440*, 297−302.

(20) Sarveswaran, K.; Gao, B.; Kim, K. N.; Bernstein, G. H.; Lieberman, M. Adhesion of DNA nanostructures and DNA origami to lithographically patterned self-assembled monolayers on Si[100]. *Proc. SPIE-Int. Soc. Opt. Eng.* **2010**, *7637*, No. 76370M.

(21) Zajac, J.; Partyka, S. In *Studies in Surface Science and Catalysis*; Dabrowski, A., Tertykh, V. A., Eds.; Elsevier: Amsterdam, 1996; Vol. *99*, pp 797−829.

(22) Kim, K. N.; Sarveswaran, K.; Mark, L.; Lieberman, M. Comparison of methods for orienting and aligning DNA origami. *Soft Matter* **2011**, *7*, 4636−4643.

(23) Hang, Q. L.; Wang, Y. L.; Lieberman, M.; Bernstein, G. H. A liftoff technique for molecular nanopatterning, . *J. Nanosci. Nanotechnol.* **2003**, *3*, 309−312.

(24) Hu, W.; Bernstein, G. H.; Sarveswaran, K.; Lieberman, M. Low temperature Development of PMMA for Sub-10-nm Electron Beam Lithography. *Proc. 3rd IEEE Conf. Nanotechnol.* **2003**, *2*, 602−605.

(25) Hu, W. C.; Sarvewsaran, K.; Lieberman, M.; Bernstein, G. Sub-10 nm electron beam lithography using cold development of poly-(methylmethacrylate). *J. Vac. Sci. Technol. B* **2004**, *22*, 1711−1716.

(26) Hu, W.; Sarveswaran, K.; Lieberman, M.; Bernstein, G. H. High resolution electron beam lithography and DNA nano-patterning for molecular QCA. *IEEE Trans. Nanotechnol.* **2005**, *4*, 312−316.

1766

dx.doi.org/10.1021/ar500001e | *Acc. Chem. Res.* 2014, 47, 1759−1767

(27) Gao, B.; Finn, M. C.; Clark, P. L.; Lieberman, M. Attachment of Salmonella phage tailspike protein to chemically modified silicon[100]. *TMS Lett.* **2004**, *1* (6), 123−124.

(28) Bernstein, G. H.; Huang, W.; Hang, Q.; Sarveswaran, K.; Lieberman, M. Electron Beam Lithography and Liftoff of Molecules and DNA Rafts. *Proc. 4th IEEE Conf. Nanosci.* **2004**, 201−203.

(29) Viot, P.; Tarjus, G.; Ricci, S. M.; Talbot, J. Random sequential adsorption of anisotropic particles. I. Jamming limit and asymptotic behavior. *J. Chem. Phys.* **1992**, *97*, 5212−5218 (see Table 2).

(30) Sarveswaran, K.; Hu, W.; Huber, P. W.; Bernstein, G. H. Deposition of DNA rafts on cationic SAMs on silicon [100]. *Langmuir* **2006**, *22*, 11279−11283.

(31) Gao, B.; Sarveswaran, K.; Bernstein, G. H.; Lieberman, M. Guided deposition of individual DNA nanostructures on silicon substrates. *Langmuir* **2010**, *26*, 12680−12683.

(32) Kim, K. N. Self-aligned DNA oligomer and the deposition of DNA oligomers on EBL patterned cationic SAMs on SiO2/Si [100]. Ph.D. Thesis, University of Notre Dame, 2012.

(33) Penzo, E.; Wang, R.; Palma, M.; Wind, S. J. Selective placement of DNA origami on substrates patterned by nanoimprint lithography. *J. Vac. Sci. Technol. B* **2011**, *29*, No. 06F205.

(34) Rothemund, P. W. K. Folding DNA to create nanoscale shapes and patterns. *Nature* **2006**, *440*, 297−302.

(35) Kershner, R. J.; Bozano, L. D.; Micheel, C. M.; Hung, A. M.; Fornof, A. R.; Cha, J. N.; Rettner, C. T.; Bersani, M.; Frommer, J.; Rothemund, P. W. K.; Wallraff, G. M. Placement and orientation of individual DNA shapes on lithographically patterned surfaces. *Nat. Nanotechnol.* **2009**, *4*, 557−561.

(36) Hung, A. M.; Micheel, C. M.; Bozano, L. D.; Osterbur, L. W.; Wallraff, G. M.; Cha, J. N. Large-area spatially ordered arrays of gold nanoparticles directed by lithographically confined DNA origami. *Nat. Nanotechnol.* **2009**, *5*, 121−126.

(37) Reichmanis, E.; Thompson, L. F. Polymer materials for microlithography. *Chem. Rev.* **1989**, *89*, 1273−1289.

(38) Shah, F. A.; Kim, K. N.; Lieberman, M.; Bernstein, G. H. Roughness optimization of electron-beam exposed hydrogen silsesquioxane for immobilization of DNA origami. *J. Vac. Sci. Technol. B* **2012**, *30*, No. 011806.

(39) Viot, P.; Tarjus, G.; Ricci, S. M.; Talbot, J. Random sequential adsorption of anisotropic particles. 1. Jamming limits and asymptotic-behavior. *J. Chem. Phys.* **1992**, *97*, 5212−5218.

(40) Levine, I. N. *Physical Chemistry*, 6th ed.; McGraw-Hill: New York, 2009; p 572.

(41) Goss, V. Adsorbing, desorbing, jamming, and burning DNA origami. Ph.D. Thesis, University of Notre Dame, 2012.

(42) Hansen, R. L.; Harris, J. M. Total internal reflection fluorescence correlation spectroscopy for counting molecules at solid/liquid interfaces. *Anal. Chem.* **1998**, *70*, 2565−2575.

(43) Hansen, R. L.; Harris, J. M. Measuring reversible adsorption kinetics of small molecules at solid/liquid interfaces by total internal reflection fluorescence correlation spectroscopy. *Anal. Chem.* **1998**, *70*, 4247−4256.

(44) Viot, P.; Tarjus, G.; Ricci, S. M.; Talbot, J. Random sequential adsorption of anisotropic particles. 1. Jamming limits and asymptotic-behavior. *J. Chem. Phys.* **1992**, *97*, 5212−5218.

(45) Ando, T. High-speed atomic force microscopy coming of age. *Nanotechnology* **2012**, *23*, No. 062001.

(46) Mangalum, A.; Rahman, M.; Norton, M. L. Site-specific immobilization of single-walled carbon nanotubes onto single and one-dimensional DNA origami. *J. Am. Chem. Soc.* **2013**, *135*, 2451−2454.

(47) Lieberman, M.; Mao, C. D.; Norton, M. Introduction to DNA Nanostructures. COLL 355, 356, 357, and 358; Presented at a Workshop at the 244th National ACS meeting, Sept. 10, 2013, Indianapolis, IN.

(48) Alloyeau, D.; Ding, B.; Ramasse, Q.; Kisielowski, C.; Lee, Z.; Jeon, K. Direct imaging and chemical analysis of unstained DNA origami performed with a transmission electron microscope. *Chem. Commun.* **2011**, *47*, 9375−9377.

(49) Yun, J. M.; Kim, K. N.; Kim, J. Y.; Shin, D. O.; Lee, W. J.; Lee, S. H.; Lieberman, M.; Kim, S. O. DNA origami nanopatterning on chemically modified graphene. *Angew. Chem., Int. Ed.* **2012**, *51*, 912−915.

(50) Lund, J.; Dong, J. C.; Deng, Z. X.; Mao, C. D.; Parviz, B. A. Electrical conduction in 7 nm wires constructed on lambda-DNA. *Nanotechnology* **2006**, *17*, 2752−2757.

(51) Park, S. H.; Prior, M. W.; LaBean, T. H.; Finkelstein, G. Optimized fabrication and electrical analysis of silver nanowires templated on DNA molecules. *Appl. Phys. Lett.* **2006**, *89*, No. 033901.

(52) Maune, H. T.; Han, S. P.; Barish, R. D.; Bokrath, M.; Goddard, W. A., III; Rothemund, P. W. K.; Winfree, E. Self-assembly of carbon nanotubes into two-dimensional geometries using DNA origami templates. *Nat. Nanotechnol.* **2009**, *5*, 61−66.

(53) Mangalum, A.; Rahman, M.; Norton, M. L. Site-specific immobilization of single-walled carbon nanotubes onto single and one-dimensional DNA origami. *J. Am. Chem. Soc.* **2013**, *135* (7), 2451−2454.

(54) Surwade, S. P.; Zhao, S.; Liu, H. Molecular lithography through DNA-mediated etching and masking of SiO$_2$. *J. Am. Chem. Soc.* **2011**, *133* (31), 11868−11871.

(55) Sivoththaman, S.; Laureys, W.; Nijs, J.; Mertens, R. Rapid thermal annealing of spin-coated phosphoric acid films for shallow junction formation. *Appl. Phys. Lett.* **1997**, *71*, 392−394.

(56) Goss, V.; Lieberman, M. DNA origami binding kinetics on mica and silicon, Oral Presentation at the American Chemical Society 244th National Meeting, COLL 465, 22 August 2012.